Epitaxial Growth of InGaN Nanowire Arrays for Light Emitting Diodes

Christopher Hahn, Zhaoyu Zhang, Anthony Fu, Cheng Hao Wu, Yun Jeong Hwang, Daniel J. Gargas, and Peidong Yang*

Department of Chemistry, University of California, Berkeley, California 94720, United States, and Materials Sciences Division, Lawrence Berkeley National Laboratory, 1 Cyclotron Road, Berkeley California 94720, United States

ABSTRACT Significant synthetic challenges remain for the epitaxial growth of high-quality InGaN across the entire compositional range. One strategy to address these challenges has been to use the nanowire geometry because of its strain relieving properties. Here, we demonstrate the heteroepitaxial growth of $In_xGa_{1-x}N$ nanowire arrays ($0.06 \leq x \leq 0.43$) on c-plane sapphire ($Al_2O_3(001)$) using a halide chemical vapor deposition (HCVD) technique. Scanning electron microscopy and X-ray diffraction characterization confirmed the long-range order and epitaxy of vertically oriented nanowires. Structural characterization by transmission electron microscopy showed that single crystalline nanowires were grown in the ⟨002⟩ direction. Optical properties of InGaN nanowire arrays were investigated by absorption and photoluminescence measurements. These measurements show the tunable direct band gap properties of InGaN nanowires into the yellow-orange region of the visible spectrum. To demonstrate the utility of our HCVD method for implementation into devices, LEDs were fabricated from $In_xGa_{1-x}N$ nanowires epitaxially grown on p-GaN(001). Devices showed blue ($x = 0.06$), green ($x = 0.28$), and orange ($x = 0.43$) electroluminescence, demonstrating electrically driven color tunable emission from this p–n junction.

KEYWORDS: InGaN nanowires · light-emitting diode · epitaxy · halide chemical vapor deposition · tunable emission

The InGaN ternary alloy has held great interest because it offers the potential for using one stable single crystalline material to obtain band gap energies from UV to IR simply by adjusting its cation stoichiometry. This large range of band gaps has made InGaN a desirable material for color tunable light-emitting/laser diodes (LED/LD).[1,2] However, the efficiencies of commercial devices quickly drop off in the green-yellow wavelength region because of current difficulties with creating single-crystalline high indium composition InGaN with a low density of dislocations.[1,2] While the exact nature of this difficulty is unknown, two factors that likely contribute are the lack of lattice-matched native substrates for the growth of InGaN and the large lattice mismatch (~10%) between GaN and InN. These strain-related factors can cause a high density of threading dislocations[1] and a large thermodynamic miscibility gap[3] for InGaN.

The nanowire geometry offers a unique platform for epitaxial alloy growth because of its strain relieving properties. Rather than releasing strain with a structural defect such as a threading dislocation, the small cross-sectional interface of nanowires can coherently relax biaxial strain from a large lattice mismatch to the substrate.[4] This is advantageous since it has been shown that the number of nonradiative recombination centers correlates with the number of threading dislocations in InGaN.[5] In addition to relieving interfacial strain, the nanowire geometry has also been conjectured to decrease alloying strain from the large lattice mismatch between InN and GaN.[6] These factors suggest that strain reduction with the nanowire geometry may play an important role in the synthesis of dislocation-free single crystalline InGaN.

Because of these advantages, InGaN-based nanowire LEDs have been made using several geometries. Most structures have incorporated radial or axial quantum wells using molecular beam epitaxy (MBE)[7] and metal–organic chemical vapor deposition (MOCVD).[8,9] Another approach is the use of single-phase $In_xGa_{1-x}N$ nanowires. Hydride vapor-phase epitaxy (HVPE) has been able to produce nanowires of $x < 0.20$, but this technique has not achieved higher indium compositions because hydrogen inhibits incorporation of indium by increasing the formation of unreactive indium species.[10] While MBE has produced nanowires of higher indium composition, the technique has relatively slow deposition rates, needs ultrahigh vacuum, and generally requires a RF source to produce the nitrogen precursor.[11,12] Therefore, the growth of InGaN nanowires by MBE would be difficult to scale for commercial production because of the cost. Although MOCVD has been commonly used to synthesize other nanowire III–V alloys because of its

* Address correspondence to p_yang@berkeley.edu.

Received for review February 8, 2011 and accepted April 15, 2011.

Published online April 15, 2011
10.1021/nn200521r

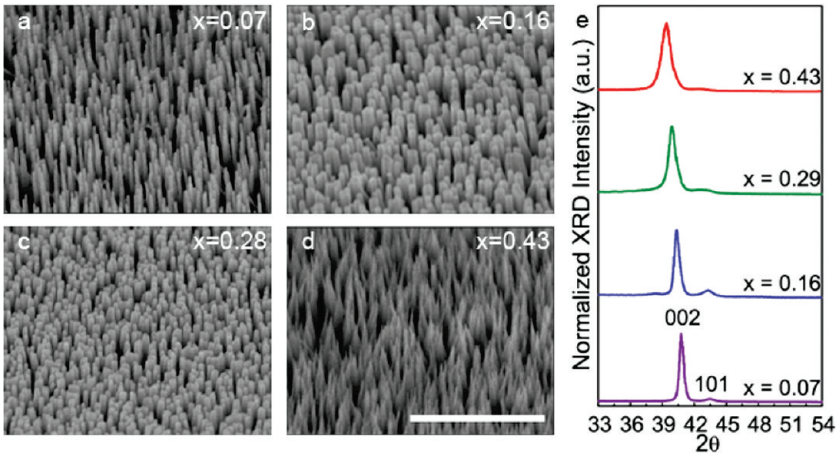

Figure 1. SEM images and XRD spectra of $In_xGa_{1-x}N$ nanowires. Tilted (45°) SEM images of $In_xGa_{1-x}N$ nanowires grown on Al_2O_3(001) where (a) $x = 0.07$, (b) $x = 0.16$, (c) $x = 0.28$, (d) $x = 0.43$. Nanowires show vertical orientation and compositions were correlated by SEM EDS. Scale bar = 1 μm. (e) XRD patterns of nanowires grown on Al_2O_3(001) display diffraction predominantly from the (002) wurtzite peak also indicating vertical orientation. Furthermore, the patterns show an increase in lattice constant with an increase in indium composition.

scalability, there have been no reports of higher indium composition ($x > 0.1$), single crystalline InGaN nanowires being produced with this technique. This may be due to the high temperatures required by MOCVD (~750−1000 °C) to reduce carbon defect incorporation from the metal−organic precursors.[13] These conditions are unfavorable for producing single crystalline high indium composition alloys because the thermal instability of InGaN can cause surface segregation of indium at these high temperatures.[14]

Recently, a breakthrough was made using a novel synthesis based on a scalable three-zone halide chemical vapor deposition (HCVD) system having the unique properties of low temperature, atmospheric pressure, and rapid growth rates.[15] By using HCVD, Kuykendall *et al*. were able to produce catalyst-free single crystalline InGaN nanowires over a broad compositional range on a single substrate. While this work demonstrated the advantage of the nanowire geometry for decreasing alloying strain, it did not address the additional challenge of strained epitaxial growth required for implementation into devices. In addition, to achieve single color electroluminsecence (EL), individual compositions of InGaN are needed rather than the compositional gradient produced by Kuykendall *et al*. Using modifications to this HCVD method, we report the heteroepitaxial growth of homogeneous InGaN nanowire arrays on Al_2O_3(001). To demonstrate the potential application of these epitaxially grown nanowire arrays, we have fabricated blue, green, and orange LEDs from InGaN nanowires on p-GaN(001).

DISCUSSION

Single-phase InGaN nanowires were grown on Al_2O_3(001) in the previously described three-zone HCVD furnace[15] using $GaCl_3$, $InCl_3$ and NH_3 as the III/V precursors (Supporting Information, Figure S1). Modifications were made to this furnace to yield nanowire arrays with homogeneous composition instead of a compositional gradient. One modification was to place both halide precursors within the same inner tube, although the precursors were still positioned in different temperature zones of the furnace. For each targeted composition, III/V ratios were adjusted by controlling the precursor temperatures and flow rates of the carrier gas (N_2) and ammonia. Growth times were relatively short (9−12 min), and nanowires typically had growth rates of *ca*. 50−100 nm/min. Low temperatures for the reaction (500−550 °C) were necessary to achieve higher indium incorporation. This temperature requirement was likely due to the formation of stable indium monochloride at higher temperatures[16] or the reduced sticking coefficient of indium at higher temperatures.[17] While the previously reported method produced mostly tapered nanowires,[15] we observed some decrease in nanowire tapering by adjusting III/V ratios. Lower ratios were found to promote nanowire growth and epitaxial growth, while higher ratios showed more tapering and thin film deposition. The morphological control using III/V ratios was analogous to what researchers have seen for the VLS growth of III−V nanowires.[18] Using these modifications, heteroepitaxial nanowire arrays of specific InGaN compositions were grown on Al_2O_3(001) .

Epitaxial growth of $In_xGa_{1-x}N$ nanowires on Al_2O_3(001) is demonstrated from scanning electron microscopy (SEM) and X-ray diffraction (XRD) characterization (Figure 1). As shown in the field-emission SEM images (Figure 1a−d), the nanowires grown on Al_2O_3(001) display a high degree of vertical orientation, indicating aligned growth from the substrate. Further characterization by XRD for fixed samples shows that the vertical arrays have the wurtzite crystal structure and show diffraction from mostly the (002) plane (Figure 1e),

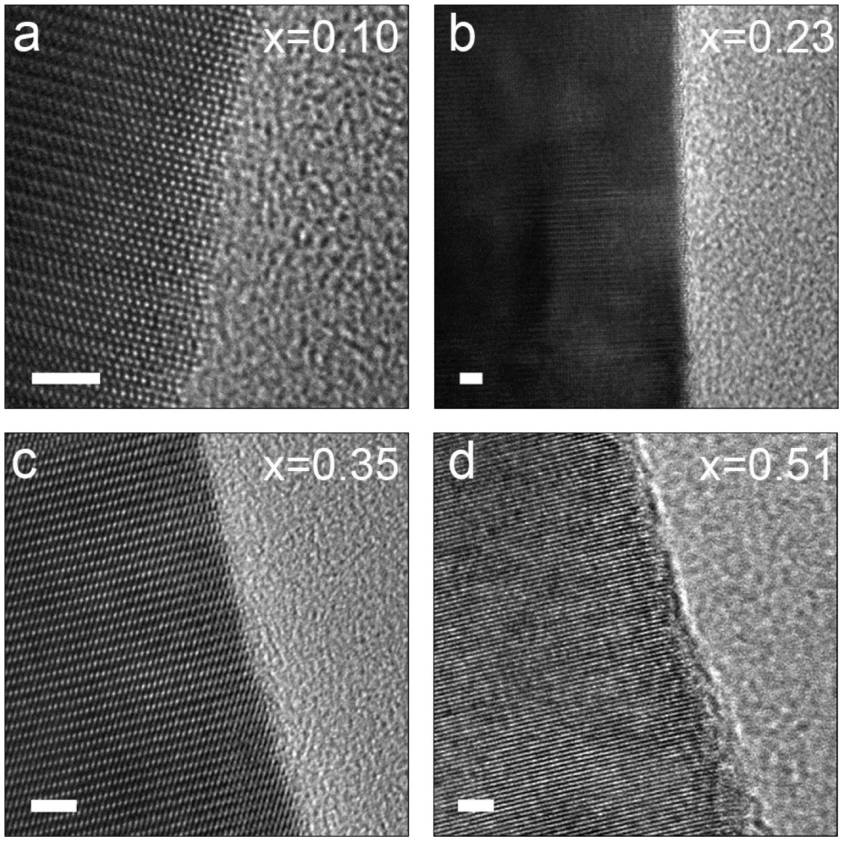

Figure 2. HRTEM images of $In_xGa_{1-x}N$ nanowires. (a–d) HRTEM images for single crystalline $In_xGa_{1-x}N$ nanowires are correlated to TEM EDS compositions. Nanowires show no indium-rich clusters and grow in the ⟨002⟩ direction. Scale bar = 2 nm.

indicating the epitaxial growth of InGaN nanowires in the ⟨002⟩ direction from Al_2O_3(001).

Samples were further analyzed by SEM energy-dispersive X-ray spectroscopy (EDS) and XRD to determine the homogeneity of vertical $In_xGa_{1-x}N$ nanowire arrays (Figure 1). Using EDS, the compositions of nanowire arrays were determined to be between $0.07 \leq x \leq 0.43$ (Figure 1a–d). Samples were mostly homogeneous over the entire substrate, with the largest compositional differences ($\Delta x < 0.04$ over 5 mm) in the direction of gas flow through the reactor. A correlation of the XRD (002) peak with the EDS composition shows a Vegard's law change in lattice constant c (Supporting Information, Figure S2a). Nanowire samples showed an increase of the (002) peak fwhm (2θ) from 0.496° for x = 0.07 to 0.983° for x = 0.43. This could be caused by alloy broadening from the random distribution of cations and bond lengths in InGaN[19] and Scherrer broadening for tapered nanowire samples. No indications of phase separation are observed in the XRD patterns.

While SEM and XRD were used to show the long-range order of the arrays, transmission electron microscopy (TEM) can be used to examine the structure of individual nanowires. High-resolution transmission electron microscopy (HRTEM) images show that the InGaN nanowires are single crystalline (Figure 2). Thermal stability differences between Ga–N and In–N bonds could cause

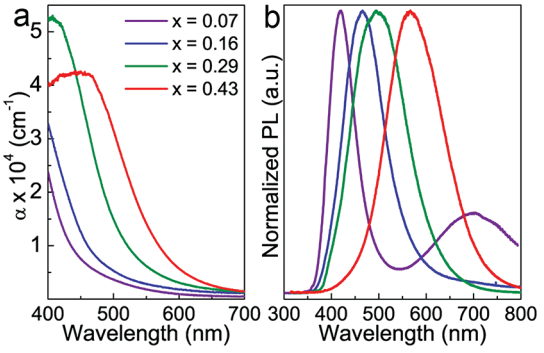

Figure 3. Absorption and PL spectra of $In_xGa_{1-x}N$ nanowire arrays. (a) Absorption spectra of nanowires taken with an integrating sphere and a 300 W Xe lamp source. Absorption coefficients were calculated by using the path length measured by cross-sectional SEM (b) PL spectra of nanowires excited by a 325 nm HeCd laser. A shift toward red wavelengths can be seen with increasing indium composition (a,b).

indium cluster formation at elevated temperatures, as well as the surface segregation of indium atoms.[14] However, no indium rich clusters were observed during growth, perhaps due to the low temperatures used. On the basis of these TEM studies, InGaN nanowires are confirmed to grow in the ⟨002⟩ direction. Since the nanowires grow vertically from Al_2O_3(001), this growth direction is expected and is also in agreement with the majority (002) peak seen in the XRD pattern.

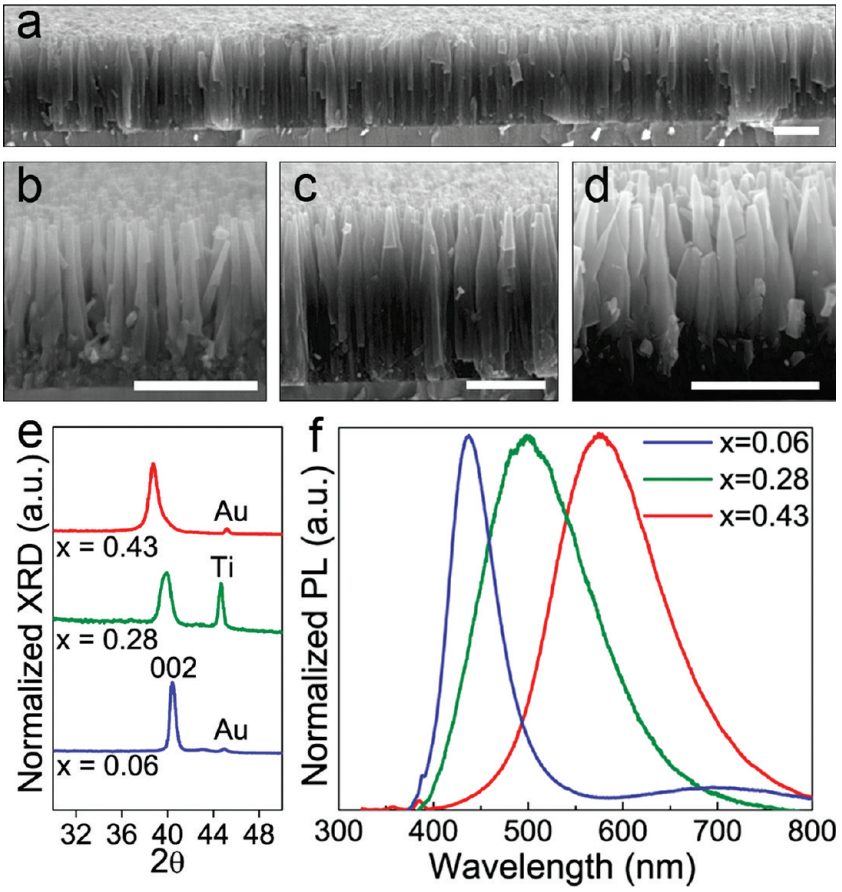

Figure 4. Cross-sectional SEM, XRD, and PL of $In_xGa_{1-x}N$ devices with $x = 0.06, 0.28, 0.43$. (a) Large-view image of $x = 0.28$ device showing uniformity. Cross-sectional SEM images of vertically grown nanowires are shown for (b) $x = 0.06$, (c) $x = 0.28$, and (d) $x = 0.43$. Scale bar = 500 nm. (e) XRD and (f) PL spectra of each device displaying no phase separation and tunable lattice constants and band gaps by adjusting the indium composition. The Au and Ti peaks present in the XRD patterns are from electrodes deposited on the nanowire arrays for electrical measurements.

Further analysis of the HRTEM images along the length of the nanowires shows whether or not dislocations are formed during heteroepitaxial growth on Al_2O_3. Two significant factors that can cause dislocation formation are the large mismatches in lattice constants and thermal expansion coefficients between Al_2O_3 and InGaN. While III-nitrides rotate 30° to adopt a less strained configuration on Al_2O_3(001),[17] the interface still has a >15% lattice mismatch to InGaN(001). Also, the large difference in thermal expansion coefficients between Al_2O_3 and InGaN creates a significant amount of tensile stress on InGaN during cooling.[20] Even with these factors, no threading dislocations were seen propagating along the length of the nanowires from TEM (Figure 2). We believe this shows the advantage of the nanowire geometry for highly lattice mismatched heteroepitaxial growth of InGaN alloys.

After structural characterization of the epitaxial $In_xGa_{1-x}N$ nanowire arrays, absorption and photoluminescence (PL) measurements were used to confirm the tunable optical properties of these alloys. Absorption spectra were taken using an integrating sphere to collect all reflected and transmitted light simultaneously from a 300 W Xe lamp source. The nanowires show a red-shift in absorption with increasing indium composition, indicating decreasing band gap energy (Figure 3a). The cross-sectional length (z) of the nanowire arrays was used to calculate an absorption coefficient (α) using the following equation: $I(z) = I_0e^{-\alpha z}$. Using a hit and miss configuration for the integrating sphere,[21] the incident and final intensities (I_0 and $I(z)$ respectively) were obtained after absorption. The calculated absorption coefficient represents the absorption properties of the InGaN nanowire ensemble system. The near band-edge absorption spectra show absorption coefficients all within the mid 10^4 cm^{-1} range 0.5 eV from the band gap, indicating strong absorption near the band edge. These absorption values are in agreement with reports stating that InGaN alloys are direct band gap.[22] Band gap values were linearly extrapolated using the square of the absorption edge (Supporting Information, Figure S2b) and are in agreement with our previous bowing equation[15] for InGaN nanowires.

To further investigate the band gap properties of epitaxially grown $In_xGa_{1-x}N$ nanowires, samples on Al_2O_3(001) were excited by a 325 nm HeCd laser to

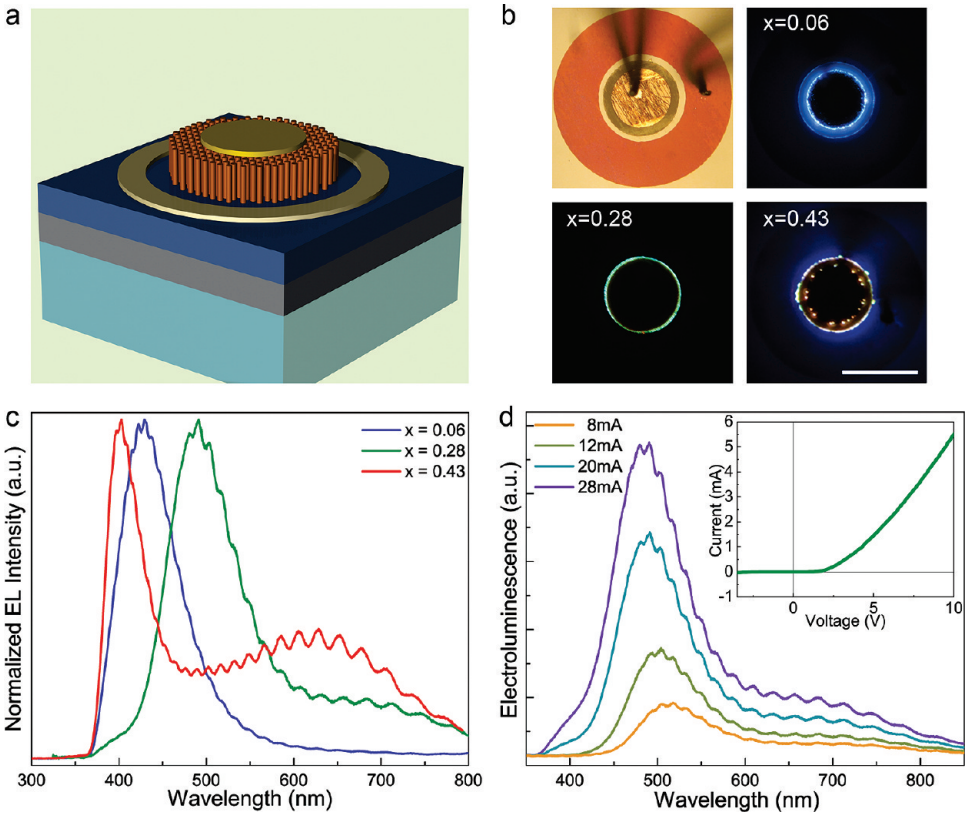

Figure 5. Characterization of $In_xGa_{1-x}N$ LEDs with $x = 0.06, 0.28, 0.43$. (a) Schematic of a fabricated LED device. The substrate is p-GaN (dark blue) grown with a GaN buffer layer (gray) on $Al_2O_3(001)$ (light blue). (b) Optical images of the devices. On the top left is a representative brightfield image of a device. Subsequent images are EL of each device under forward bias ($V = 19$, 9, and 11 V for $x = 0.06$, 0.28, and 0.43, respectively) demonstrating tunable emission. Scale bar = 250 μm. (c) Normalized EL spectra of each device in panel b. (d) Dependence of EL on current of $x = 0.28$ device. Inset: Typical $I-V$ curve showing rectification.

measure the PL (Figure 3b). Similar to the absorption spectra, a red-shift in emission energy can be seen from an increase in indium composition. The emission energies analyzed from PL spectra demonstrate the ability to tune InGaN emission into the yellow-orange region of the visible spectrum using heteroepitaxially grown nanowires. A comparison between the absorption and PL spectra reveals that the nanowires display a slight Stokes shift in emission from the absorption edge (Supporting Information, Figure S2b). In addition, the line width of the PL spectra may be attributed to the extent of short-range disorder of cations in InGaN. These atomic-scale compositional fluctuations can cause alloy broadening of the emission from localized energy states.[23]

To demonstrate the potential utility of epitaxially grown single-phase InGaN nanowire arrays, LEDs were fabricated from n-type arrays grown on p-GaN(001). The nanowires were grown within 250 μm diameter circles on p-GaN substrates (1 μm thick p-GaN and 2 μm thick undoped GaN buffer on $Al_2O_3(001)$) that were cleaned with HCl/DI H_2O (1:1)). A representative large-area cross-sectional SEM image (Figure 4a) shows that the wire growth is relatively uniform. As with growth on $Al_2O_3(001)$, SEM images (Figures 4b–d) and XRD patterns (Figure 4e) confirm the vertical alignment of the nanowires for all indium compositions produced suggesting epitaxial growth along the *c*-axis. XRD patterns and PL spectra (Figure 4f) for each sample demonstrate tunable lattice constants and band gaps by tuning the indium content. The PL peak wavelengths were 435, 500, and 575 nm for $x = 0.06$, 0.28, and 0.43, respectively. Dislocation analysis at the InGaN–GaN interface was not performed in this study.

Optical characterization of each device under forward bias showed EL emission that was tunable by adjusting the indium composition. A schematic of the LED device structure (Figure 5a) shows a Ni/Au electrode surrounding the array to make contact to the p-GaN. A circular Ti/Au metal electrode was deposited on top of the array. All nanowires were electrically connected to each other at the base of the array (Figures 4a–d), resembling a continuous thin film with columnar nanostructures. A representative top-view image of a fabricated LED device and forward-biased EL images of each device were taken with a digital camera (Figure 5b). Blue (~430 nm), green (~500 nm), and orange (~620 nm) emissions from the nanowire areas were observed for devices with indium compositions $x = 0.06$, $x = 0.28$, and $x = 0.43$, respectively. The

colors seen in Figure 5b correspond to the EL peaks in Figure 5c. The blue and green peaks of the $x = 0.06$ and $x = 0.28$ devices match the corresponding PL peaks in Figure 4f, demonstrating consistency between the two different emission mechanisms. The orange EL peak for the $x = 0.43$ device, however, is red-shifted 45 nm from the corresponding PL, indicating possible compositional and strain differences at the interface. In the EL spectra of the $x = 0.28$ and 0.43 devices, a 400 nm peak is present and is likely from electron injection into the substrate, as evidenced by its insensitivity to the changes in nanowire composition and by the blue emission's location outside the nanowire growth region in the image of the $x = 0.43$ device. Other notable features of the EL spectra include increasing optical line width with increasing indium composition indicative of alloy broadening[24,25] and small oscillations likely due to Fabry–Perot interference of the two interfaces in the 3 μm GaN thin film.

Further LED characterization revealed that the emission's dependence on current for the $x = 0.28$ device displays slight blue shifting with increasing current and the diode shows rectification (Figure 5d). The EL spectra show the peak at ~500 nm blue shifting 30 nm when the injection current increases from 8 to 28 mA. This result further suggests possible alloy broadening and band-tail filling,[26,27] and is in agreement with the broadening seen in the XRD pattern and PL spectrum. The current–voltage (I–V) curve in the inset demonstrates rectifying behavior for these devices with turn-on voltages around 2 V and relatively small leakage current at reverse bias. The current–voltage behavior and current dependent emission for $x = 0.06$ and 0.43 can be seen within the Supporting Information (Figures S3,S4).

CONCLUSIONS

Using a modified HCVD approach, we were able to produce large area homogeneous $In_xGa_{1-x}N$ nanowire arrays up to $x = 0.43$ by using a simple, fast, and uniform growth technique. Epitaxial growth was demonstrated on both Al_2O_3(001) and p-GaN(001) using XRD and SEM, showing the utility of this HCVD method. Further characterization by TEM confirmed the growth of single crystalline nanowires in the ⟨002⟩ direction from the substrate and a lack of threading dislocations. We believe this shows that nanowires are a viable geometry for the epitaxial growth of high indium composition InGaN. Three LED devices were fabricated from nanowires grown on p-GaN(001), and demonstrate tunable color electroluminescence from blue to orange with increasing indium composition. Future work will be done to measure the quantum efficiency of InGaN nanowire LEDs and to increase the indium composition of the devices to achieve the full color range of LEDs. The epitaxial growth of InGaN nanowires with HCVD was an important step toward device implementation not only in our LEDs but also toward future applications such as photovoltaics and photoelectrochemistry.

EXPERIMENTAL SECTION

Modifications to the combinatorial setup[15] were made to synthesize homogeneous arrays of epitaxial InGaN nanowires on Al_2O_3(001) and p-GaN(001). A schematic of the three-zone HCVD system is shown in the Supporting Information (Figure S1). This system has three $^1/_4$-in. quartz tubes enclosed in a 1-in. quartz tube. For homogeneous growth, only two of the inner tubes were used for delivering the III–V precursors. The temperature along the inner tubes was controlled separately by two furnaces equipped with three thermocouples (zones 1–3). The $GaCl_3$ (99.999% metals basis, Alfa Aesar) and $InCl_3$ (99.999% metals basis, Alfa Aesar) solid precursors were loaded into the same inner quartz tube within a glovebox and sealed for transfer. The solid precursors were spaced within this inner tube such that their vapor pressures could be controlled separately in zone 1 and zone 2, respectively, and N_2 was used as a carrier gas. Substrates were placed flat on a quartz plate 1–3 cm from the end of this inner tube. By controlling the temperatures of zone 1 ($GaCl_3$, 65–70 °C) and zone 2 ($InCl_3$, 320–435 °C) as well as the N_2 (15 sccm for precursor tube, 300 sccm for outer tube), and NH_3 (110–150 sccm) flow rates, the $In_xGa_{1-x}N$ composition could be rationally tuned ($0.07 \leq x \leq 0.43$). The temperature in zone 3 was held constant at 730 °C, and the reaction temperature varied based on the substrate's position (500–550 °C) within the temperature gradient of the furnace. The reaction proceeded for 9–12 min.

XRD patterns were taken using a Bruker AXS D8 Advance diffractometer, which used an incident Co Kα radiation of 1.79026 Å. Spectra were collected by fixing samples onto a flat puck. HRTEM images were taken using a JEOL JEM-2100 LaB6 microscope at 200 kV. The microscope was equipped with an Oxford EDS detector, and EDS data were collected from the Ga K and the In L peaks of single nanowires. SEM images and correlated EDS spectra were taken using a JEOL JSM-6340F field emission scanning electron microscope equipped with an EDAX Falcon detector. EDS data were collected from the Ga K and the In L peaks of a 40 μm × 40 μm area for each sample at 20 kV and analyzed using the software's true standardless-quantification mode. The indium compositions of each LED device were measured with each sample at a 45° tilt. The presented number should be a lower limit to the actual composition.

Absorption spectra were collected using a custom 4-in. diameter integrating sphere (Gigahertz Optik UPK-100-L coated with ODM98) and a Newport 300 W Xe arc lamp as a broadband light source. Signals were sent to a liquid N_2 (LN) cooled CCD/spectrometer (PI Acton) *via* an optical fiber. Samples were placed on a holder in the center of the integrating sphere at a slight angle. An iris was used to decrease the beam-spot to the same size or smaller than the sample. Absorption was measured using a hit and miss method described elsewhere.[21] PL and EL spectra were collected through a 50× objective on a Nikon microscope and routed to the LN cooled CCD/spectrometer. LED devices were characterized (I–V and EL) using a home-built probe station integrated with the Nikon microscope and a semiconductor parameter analyzer (Agilent 4155C).

LEDs were fabricated from nanowires grown on p-GaN(001). A 1 μm plasma-enhanced CVD SiO_2 mask was deposited on a 1 cm × 5 mm substrate. Several 250 μm diameter windows were opened in the mask by standard photolithography techniques and a ~15–20 min HF/H_2O (1:10) etch, and the residual photoresist was removed with piranha. The substrate was cleaned with HCl/H_2O (1:1) for 1 min before HCVD growth. Following the growth of the nanowires, the SiO_2 mask was removed with HF/H_2O (1:10). Metal contacts were deposited

using standard photolithography techniques and an e-beam evaporator. Ni/Au (20 nm/20 nm) contacts were deposited on p-GaN (Supporting Information, Figure S5) and annealed in a rapid thermal annealing furnace for 1 min at 500 °C in O_2 before Ti/Au (50 nm/50 nm) contact deposition on the array. The separation between the edge of the array and the inner edge of the Ni/Au contact was 25 μm. Small separation distances allowed for a higher current density at the nanowire/p-GaN interface and limited the effect of parasitic current paths due to voltage drops across the internal junction within the substrate.

Acknowledgment. This work was supported by the Director, Office of Science, Office of Basic Energy Sciences, Materials Sciences and Engineering Division, of the U.S. Department of Energy under Contract No. DE-AC02-05CH11231. The work on LED devices is supported by Samsung. We thank the National Center for Electron Microscopy for the use of their facilities. The Samsung Advanced Institute of Technology provided the p-GaN used in this experiment. Special thanks to Tev Kuykendall, Shaul Aloni, and Sarah Brittman for scientific discussion.

Supporting Information Available: Experimental set up for HCVD and additional *I*–*V* and EL data. This material is available free of charge *via* the Internet at http://pubs.acs.org.

REFERENCES AND NOTES

1. Phillips, J. M.; Coltrin, M. E.; Crawford, M. H.; Fischer, A. J.; Krames, M. R.; Mueller-Mach, R.; Mueller, G. O.; Ohno, Y.; Rohwer, L. E. S.; Simmons, J. A.; *et al*. Research Challenges to Ultraefficient Inorganic Solid-State Lighting. *Laser Photon. Rev.* **2007**, *1*, 307–333.
2. Khan, A. Semiconductor Photonics: Laser Diodes Go Green. *Nat. Photon.* **2009**, *3*, 432–434.
3. Stringfellow, G. B. Microstructures Produced during the Epitaxial Growth of InGaN Alloys. *J. Cryst. Growth* **2010**, *312*, 735–749.
4. Ertekin, E.; Greaney, P. A.; Chrzan, D. C.; Sands, T. D. Equilibrium Limits of Coherency in Strained Nanowire Heterostructures. *J. Appl. Phys.* **2005**, *97*, 114325.
5. Chichibu, S. F.; Uedono, A.; Onuma, T.; Sota, T.; Haskell, B. A.; DenBaars, S. P.; Speck, J. S.; Nakamura, S. Limiting Factors of Room-Temperature Nonradiative Photoluminescence Lifetime in Polar and Nonpolar GaN Studied by Time-Resolved Photoluminescence and Slow Positron Annihilation Techniques. *Appl. Phys. Lett.* **2005**, *86*, 021914.
6. Xiang, H. J.; Wei, S. H.; Da Silva, J. L. F.; Li, J. B. Strain Relaxation and Band-Gap Tunability in Ternary $In_xGa_{1-x}N$ Nanowires. *Phys. Rev. B* **2008**, *78*, 193301.
7. Armitage, R.; Tsubaki, K. Multicolour Luminescence from InGaN Quantum Wells Grown over GaN Nanowire Arrays by Molecular-Beam Epitaxy. *Nanotechnology* **2010**, *21*, 195202.
8. Qian, F.; Gradecak, S.; Li, Y.; Wen, C. Y.; Lieber, C. M. Core/Multishell Nanowire Heterostructures as Multicolor, High-Efficiency Light-Emitting Diodes. *Nano Lett.* **2005**, *5*, 2287–2291.
9. Kim, H. M.; Cho, Y. H.; Lee, H.; Kim, S. I.; Ryu, S. R.; Kim, D. Y.; Kang, T. W.; Chung, K. S. High-Brightness Light Emitting Diodes Using Dislocation-Free Indium Gallium Nitride/Gallium Nitride Multiquantum-Well Nanorod Arrays. *Nano Lett.* **2004**, *4*, 1059–1062.
10. Hwa-Mok, K.; Hosang, L.; Suk Il, K.; Sung Ryong, R.; Tae Won, K.; Kwan Soo, C. Formation of InGaN Nanorods with Indium Mole Fractions by Hydride Vapor Phase Epitaxy. *Phys. Status Solidi B* **2004**, *241*, 2802–2805.
11. Guo, W.; Zhang, M.; Banerjee, A.; Bhattacharya, P. Catalyst-Free InGaN/GaN Nanowire Light Emitting Diodes Grown on (001) Silicon by Molecular Beam Epitaxy. *Nano Lett.* **2010**, *10*, 3355–3359.
12. Vajpeyi, A. P.; Ajagunna, A. O.; Tsagaraki, K.; Androulidaki, M.; Georgakilas, A. InGaN Nanopillars Grown on Silicon Substrate Using Plasma Assisted Molecular Beam Epitaxy. *Nanotechnology* **2009**, *20*, 325605.
13. Koleske, D. D.; Wickenden, A. E.; Henry, R. L.; Twigg, M. E. Influence of MOVPE Growth Conditions on Carbon and Silicon Concentrations in GaN. *J. Cryst. Growth* **2002**, *242*, 55–69.
14. Chen, H. J.; Feenstra, R. M.; Northrup, J. E.; Zywietz, T.; Neugebauer, J. Spontaneous Formation of Indium-Rich Nanostructures on InGaN(0001) Surfaces. *Phys. Rev. Lett.* **2000**, *85*, 1902–1905.
15. Kuykendall, T.; Ulrich, P.; Aloni, S.; Yang, P. Complete Composition Tunability of InGaN Nanowires Using a Combinatorial Approach. *Nat. Mater.* **2007**, *6*, 951–956.
16. Kumagai, Y.; Takemoto, K.; Koukitu, A.; Seki, H. Thermodynamics on Halide Vapor-Phase Epitaxy of InN Using InCl and $InCl_3$. *J. Cryst. Growth* **2001**, *222*, 118–124.
17. Jain, S. C.; Willander, M.; Narayan, J.; Van Overstraeten, R. III-Nitrides: Growth, Characterization, and Properties. *J. Appl. Phys.* **2000**, *87*, 965–1006.
18. Joyce, H. J.; Gao, Q.; Tan, H. H.; Jagadish, C.; Kim, Y.; Fickenscher, M. A.; Perera, S.; Hoang, T. B.; Smith, L. M.; Jackson, H. E.; *et al*. Unexpected Benefits of Rapid Growth Rate for III–V Nanowires. *Nano Lett.* **2009**, *9*, 695–701.
19. Mattila, T.; Zunger, A. Predicted Bond Length Variation in Wurtzite and Zinc-Blende InGaN and AlGaN Alloys. *J. Appl. Phys.* **1999**, *85*, 160–167.
20. Liu, L.; Edgar, J. H. Substrates for Gallium Nitride Epitaxy. *Mater. Sci. Eng. R-Rep* **2002**, *37*, 61–127.
21. Hanssen, L. Integrating-Sphere System and Method for Absolute Measurement of Transmittance, Reflectance, and Absorptance of Specular Samples. *Appl. Opt.* **2001**, *40*, 3196–3204.
22. Wu, J.; Walukiewicz, W.; Yu, K. M.; Shan, W.; Ager, J. W.; Haller, E. E.; Lu, H.; Schaff, W. J.; Metzger, W. K.; Kurtz, S. Superior Radiation Resistance of $In_{1-x}Ga_xN$ Alloys: Full-Solar-Spectrum Photovoltaic Material System. *J. Appl. Phys.* **2003**, *94*, 6477–6482.
23. Singh, J.; Bajaj, K. K. Theory of Excitonic Photoluminescence Linewidth in Semiconductor Alloys. *Appl. Phys. Lett.* **1984**, *44*, 1075–1077.
24. Schubert, E. F., *Light-Emitting Diodes;* Cambridge University Press: U.K., 2006.
25. Bertram, F.; Srinivasan, S.; Liu, R.; Geng, L.; Ponce, F. A.; Riemann, T.; Christen, J.; Tanaka, S.; Omiya, H.; Nakagawa, Y. Spatial Variation of Luminescence of InGaN Alloys Measured by Highly-Spatially-Resolved Scanning Cathodoluminescence. *Mater. Sci. Eng. B* **2002**, *93*, 19–23.
26. Chichibu, S.; Azuhata, T.; Sota, T.; Nakamura, S. Spontaneous Emission of Localized Excitons in InGaN Single and Multiquantum Well Structures. *Appl. Phys. Lett.* **1996**, *69*, 4188–4190.
27. Kuokstis, E.; Yang, J. W.; Simin, G.; Khan, M. A.; Gaska, R.; Shur, M. S. Two Mechanisms of Blueshift of Edge Emission in InGaN-Based Epilayers and Multiple Quantum Wells. *Appl. Phys. Lett.* **2002**, *80*, 977–979.